

Reduced pH and contractility in failing rat cardiomyocytes

O. J. Kemi,^{1,2} I. Arbo,¹ M. A. Høydal,¹ J. P. Loennechen,³ U. Wisløff,^{1,3} G. L. Smith² and Ø. Ellingsen^{1,3}

¹ Department of Circulation and Medical Imaging, Faculty of Medicine, Norwegian University of Science and Technology, Trondheim, Norway

² Institute of Biomedical and Life Sciences, University of Glasgow, Glasgow, UK

³ Department of Cardiology, St Olavs Hospital, Trondheim, Norway

Received 1 March 2005,
revision requested 20 April 2005
final revision received 15 July
2006,
accepted 20 August 2006
Correspondence: Ø. Ellingsen,
Department of Circulation and
Medical Imaging, Medical
Technology Research Centre,
Olav Kyrres gate 9, NO-7489
Trondheim, Norway. E-mail:
oyvind.ellingsen@ntnu.no

Abstract

Aim: To determine whether reduced cardiomyocyte contractility in heart failure is associated with reduced intracellular pH (pH_i). Involvement of the Na^+/H^+ exchanger and the H^+/K^+ ATPase were investigated with specific blockers.

Methods: Myocardial infarction and subsequent heart failure in Sprague–Dawley rats were induced by chronic occlusion of the left coronary artery. 6 weeks post-ligation, contractility (cell shortening) and pH_i (BCECF fluorescence) were recorded in freshly dissociated cardiomyocytes during 2–10 Hz electrical stimulation, with or without either Na^+/H^+ exchanger or H^+/K^+ ATPase inhibition.

Results: Elevated end-diastolic and reduced peak systolic pressures confirmed heart failure. Increased heart weights (20–30%; $P \leq 0.01$) and cardiomyocyte lengths and widths (22–25%; $P \leq 0.01$) confirmed substantial cardiac hypertrophy. In myocytes isolated from sham operated rats, a positive staircase response occurred with stimulation rates from 2 to 7 Hz; further increases in stimulation rate up to 10 Hz reduced contractility. In contrast, pH_i fell progressively over the entire stimulation range. In failing myocytes, pH_i was consistently 0.07 pH units lower and contractility 40% lower ($P \leq 0.01$) than sham control values; the shape of the contractility staircase remained similar to controls. At all stimulation frequencies, Na^+/H^+ exchanger inhibition reduced pH_i by 0.05 pH units ($P \leq 0.01$) and contractility by 22% ($P \leq 0.05$) in cardiomyocytes from the heart failure group. A significantly smaller decrease of pH_i and reduction in contractility was observed after inhibition of Na^+/H^+ exchanger (10 μM HOE694) in sham myocytes. H^+/K^+ ATPase inhibition (100 μM SCH28080) had no effect on pH_i .

Conclusion: Reduced pH_i is accompanied by reduced cardiomyocyte contractility in isolated myocytes from post-MI heart failure. The data suggest compensatory Na^+/H^+ exchanger activation in heart failure, whereas H^+/K^+ ATPase does not appear to contribute significantly to pH_i maintenance.

Keywords cardiac, contractility, heart failure, myocytes, Na^+/H^+ exchanger-1, pH.

Depressed contractile function in cardiomyocytes is a central feature in heart failure (Gwathmey *et al.* 1990, Perez *et al.* 1999). Whereas defective Ca^{2+} cycling is

perhaps the most important mechanism, controversy remains over the contribution of altered myofilament Ca^{2+} sensitivity to depressed contractility (Gwathmey

& Hajjar 1990). Nonetheless, novel inotropes based on enhancement of cardiac myofilament sensitivity to Ca^{2+} are improving clinical outcome in heart failure (Hasenfuss *et al.* 1998, Brixius *et al.* 2002, Lehmann *et al.* 2003). Previous studies from our laboratory demonstrated that depressed contractility and Ca^{2+} sensitivity coincide with depressed tolerance to acidosis in heart failure (Loennechen *et al.* 2002, Wisløff *et al.* 2002), whereas Ca^{2+} sensitivity correlates well with intracellular pH (pH_i) in non-failing cardiomyocytes (Wisløff *et al.* 2002). Inter-dependence between pH_i and contractile function is already well established in healthy hearts (Blanchard & Solaro 1984), at least partly because low pH_i reduces Ca^{2+} binding to troponin C; thus reducing Ca^{2+} sensitivity. Such inter-dependence may also contribute to lower contractility in heart failure. So far, low pH_i has only been described in pressure-overload hypertrophy (Wallis *et al.* 1997). Hence, one aim of the present study was to determine whether reduced contractility in heart failure is associated with depressed pH_i .

A second aim was to investigate involvement of Na^+/H^+ exchanger-1 (NHE-1) and H^+/K^+ ATPase (HKA) on pH_i and contractile function by the specific inhibitors HOE 694 and SCH 28080 respectively. Both NHE-1, the main sarcolemmal proton extruder, and HKA increase expression and/or activity in heart failure, which may indicate regulatory functions (Karmazyn *et al.* 1999, Loennechen *et al.* 2002, Beisvag *et al.* 2003, Chen *et al.* 2004). Until recently, the existence of cardiac HKA was debated, until expression and functional activity assays brought evidence of its presence both in the ventricle and atrium (Nagashima *et al.* 1999, Beisvag *et al.* 2003, Yenisehirli & Onur 2005). Since various buffer systems, like the $\text{Na}^+/\text{HCO}_3^-$ symport and intracellular cytoplasmic and extrinsic $\text{CO}_2/\text{HCO}_3^-$ buffers also influence pH_i -optimum (Leem *et al.* 1999, Zaniboni *et al.* 2003), experiments were performed in $\text{CO}_2/\text{HCO}_3^-$ -buffered Tyrode solution, and confirmed in *N*-2-hydroxyethylpiperazine-*N'*-2-ethane sulphonic acid (HEPES) solutions.

Materials and methods

Animals and study design

Female adult Sprague–Dawley rats (Møllegaards Breeding Centre, Lille Skensved, Denmark), weighing 240 ± 10 g at inclusion were housed in a 12 : 12 h light and dark cycle; a pellet rodent diet and water were given *ad libitum*. Animals were randomized to either experimentally induced myocardial infarction or sham surgery; left ventricular and aortic pressures were recorded 5 weeks later to confirm heart failure, whereas

after 6 weeks, animals were killed and the hearts removed for cardiomyocyte isolation. The Norwegian Council for Animal Research approved experimental protocols, which conformed to the *European Convention for the Protection of Vertebrate Animals Used for Experimental and Other Scientific Purposes* (Council of Europe no. 123, Strasbourg 1985).

Myocardial infarction

Experimental infarctions were induced as previously described (Loennechen *et al.* 2001). Briefly, animals were anaesthetized with a 3 : 7 mixture of $\text{O}_2/\text{N}_2\text{O}$ and 5% isoflurane (Abbot Scandinavia, Solna, Sweden) and intubated with a volume-controlled ventilator (Model 655; Harvard Apparatus, Edenbridge, UK), and ventilated with a 3 : 7 mixture of $\text{O}_2/\text{N}_2\text{O}$ and 1% isoflurane. A left thoracotomy in the fifth intercostal space was performed. The pericardium was removed and the heart was exposed, whereupon the left coronary artery was ligated with a polyester suture (Ethibond 6–0 with a RB-2 needle; Ethicon, Norderstedt, Germany). Sham-operated controls underwent the same surgical procedures, except coronary artery ligation. All animals were given 0.05 mg buprenorphin (0.3 mg mL^{-1} Temgesic, Reckitt and Coleman, Hull, UK) subcutaneously immediately and 10 h post-surgery. All sham-operated animals and 30% of the MI-operated animals survived for inclusion in the study; thus, the MI and sham groups both proceeded with 11 animals in each.

Echocardiography and in vivo pressure measurements

A week after surgery, 2D short-axis echocardiography (10 MHz linear array probe, System Five ultrasound scanner, GE Vingmed Ultrasound, Horten, Norway) was performed after intraperitoneal sedation with 40 mg kg^{-1} ketamine hydrochloride and 8 mg kg^{-1} xylazine in a cohort of animals ($n = 5$), to estimate the infarct size by measuring the percentage infarcted area of total endocardial circumference (Litwin *et al.* 1994). For intracardiac pressure recordings, animals were anaesthetized and ventilated as during MI or sham operations. The right carotid artery was exposed and cannulated with a 2-Fr-sized pressure microtip catheter (Model SPR 407; Millar Instruments, Houston, TX, USA), which was advanced into the aorta and left ventricle (LV) for measuring systolic and diastolic pressures. LV end-diastolic pressure (LVEDP) and LV peak systolic pressure (LVPS), as well as aortic diastolic and systolic pressures were calculated as the means of 10 consecutive pressure cycles. On completion of the recordings, the artery was ligated and animals received post-surgery treatment similar to post-MI and sham operations (buprenorphin).

Cardiomyocyte isolation

Under full ether anaesthesia, animals were heparinized (0.2 mL of 1000 IU mL⁻¹ heparin; Novo Nordisk, Copenhagen, Denmark) and cardiomyocytes were isolated as previously described (Loennechen *et al.* 2001) with a modified Krebs–Henseleit Ca²⁺ free buffer in a retrograde Langendorff perfusion system. Collagenase type II (250 IU mL⁻¹; Worthington, Freeland, NJ, USA) and CaCl₂ stepwise to 1.2 mM were subsequently introduced. After perfusion, ventricles were weighed and the infarct area was removed; thus, LV cardiomyocytes remote to the infarct area were processed for cell measurements. Cardiomyocytes were deposited on laminin-coated (10 mg mL⁻¹; Life Technologies, Paisley, UK) coverslips in a CO₂/HCO₃⁻-buffered or HEPES-buffered (control experiments in the absence of CO₂/HCO₃⁻) Tyrode solution until microscopy measurements were performed later the same day.

Cardiomyocyte contractility, pH_i, and size

For contractility and pH_i measurements, cells were placed in a closed chamber (37 °C, HCO₃⁻-buffered Tyrode solution continuously equilibrated with 5% CO₂) on an inverted microscope (Diaphot-TMD, Nikon, Tokyo, Japan) converted to epifluorescence, and stimulated electrically by bipolar pulses as previously described (Wisløff *et al.* 2001). Cell shortening and relaxation were measured by video edge-detection (Model 104; Crescent Electronics, Sandy, UT, USA). Ten stable, consecutive contraction cycles at each stimulation frequency (2, 5, 7 and 10 Hz, and thereafter at 1 Hz to ensure intact cells) were studied in four to six cells per animal in each condition (Tyrode, Tyrode + HOE 694, Tyrode + SCH 28080; see next section). pH_i measurements were performed after BCECF-AM loading with a 100 Hz rotating mirror alternating excitation wavelength through band-pass filters of 440 and 490 nm, with background fluorescence being measured and subtracted for each cell. Fluorescence emission at 525 nm was counted with a photomultiplier tube (D-104; Photon Technology International, Lawrenceville, NJ, USA). In each animal, four to six cells per condition (Tyrode, Tyrode + HOE 694, Tyrode + SCH 28080; see next section) were studied at increasing stimulation frequencies (2, 5, 7 and 10 Hz). Each frequency was maintained until pH_i stabilized, usually within 2–3 min. In addition, experiments were repeated in HEPES-buffered Tyrode to exclude possible effects of HCO₃⁻ that would also have the potential to alter pH_i. After the final stimulation protocol in each condition, calibration was performed by perfusing cells with the ionophore nigericin, which equilibrates

extra- and intracellular pH_i (pH values 7.5, 7.0 and 6.5; see next section for solution details). pH_i was determined from linear regressions of fluorescence ratio vs. the pH_i values. From each animal, 100 cells without visible cellular damage were measured for length and midpoint width. Cell volume (in pL) was calculated as cell length × width × 0.00759, as established by 2D light and 3D confocal microscopy (Sato *et al.* 1996).

Solutions and pH_i calibration

After isolation, cells rested in CO₂/HCO₃⁻-buffered Tyrode solution containing (in mM) 117 NaCl, 23 NaHCO₃, 5.4 KCl, 1.2 CaCl₂, 1.2 MgCl₂, and 11 Glucose, or HEPES-buffered Tyrode in which NaHCO₃ was replaced by 10 mM HEPES; both solutions equilibrated with 5% CO₂, pH 7.4, 37 °C, before being subjected to different protocols later the same day. The batches intended for pH_i measurements were loaded for 20 min with 2 μM of the pH-sensitive fluorescent dye 2',7'-bis-(2-carboxyethyl)-5-(6) carboxyfluorescein acetoxymethyl ester (BCECF-AM; Molecular Probes, Eugene, OR, USA) and 0.3% dimethyl sulphoxide (DMSO; Sigma Chemical, St Louis, MO, USA) in room temperature, and subsequently washed.

Calibration buffers for pH_i 7.5 and 7.0 consisted of (in mM) 140 KCl, 1 MgCl₂, 8 Glucose, 10 HEPES, 1 EGTA and 7 μM Nigericin. For the pH_i 6.5 buffer, HEPES was replaced by 10 mM MES. pH was adjusted with KOH or HCl. After each calibration procedure, the cell chamber and superfusion system were carefully washed to prohibit nigericin contamination during cell measurements.

Inhibition of specific pH_i regulation systems

For contractility and pH_i measurements, cells were divided into one of the following batches: (1) remained in CO₂/HCO₃⁻-buffered or HEPES-buffered Tyrode vehicle solution throughout the experiment; or (2) subject to specific inhibition of NHE-1 with 10 μM HOE 694 (HOE 694 was provided by Hoechst Marion Roussel, Frankfurt am Main, Germany as a kind gift) for 20 min and throughout the experiment; or (3) inhibition of HKA with 100 μM SCH 28080 (Schering-Plough Research Institute, Kenilworth, NJ, USA) for 20 min and throughout the experiment. HOE 694, structurally similar to HOE 642 (Cariporide) and SCH 28080 were added to Tyrode vehicle 20 min before microscopy, and remained throughout experiment (together with BCECF-AM for pH measurements). The final inhibitor solutions were chosen on the basis of previous experiments (Beisvag *et al.* 2003, Teshima *et al.* 2003).

Statistics

Data are expressed as mean \pm SD and $P < 0.05$ determined statistical significance. The Mann–Whitney test determined differences between groups, whereas a univariate repeated-measures ANOVA test verified differences and investigated differences between the curve-shapes during increasing stimulation frequencies (cell contractility and pH). Relationships were assessed by Pearson's correlation coefficients and complementary univariate backward linear multiple regression analyses, with fractional shortening at 7 Hz as the dependent variable, pH_i , myocyte dimensions, and heart and ventricle weights and pressures as the independent variables, and $P > 0.05$ as exclusion criterion. Forward regression analysis did not yield different conclusions than the backward approach, and is therefore not presented.

Results

Left ventricular pressures and cardiac hypertrophy

Heart failure post-MI was confirmed by *in vivo* LV pressure recordings. LVEDP was substantially elevated in failure animals; all well above the selection criterion of 15 mmHg and thus confirming heart failure, whereas LVPSP decreased by 24 mmHg (Table 1). Infarct size was estimated to $40 \pm 5\%$. Heart weights increased approx. 20–30%, LV approx. 30%, and the right ventricle (RV) approx. 18%; however, when related to body mass, only heart and LV weights increased (Table 2). Pathological hypertrophy was also confirmed by cellular growth; left ventricular cardiomyocyte length increased by 22% and width by 25%, which resulted in 58% larger estimated cell volumes.

Cardiomyocyte contractility and pH_i

pH_i and contractile responses to electrical stimulation up to physiological frequencies were markedly different between sham and heart failure. Fractional shortening

Table 1 Left ventricle and aortic pressures

	Control	Heart failure
LV end-diastolic pressure (mmHg)	5 \pm 3	22 \pm 5*
LV peak systolic pressure (mmHg)	116 \pm 17	92 \pm 22**
Aortic diastolic pressure (mmHg)	70 \pm 19	80 \pm 22

Data are mean \pm SD, $n = 11$ in each group.

LV, left ventricle. Elevated (>15 mmHg) LV end-diastolic pressure indicates heart failure.

Differences between control and heart failure: * $P < 0.01$;

** $P < 0.05$.

was approx. 40% less in failing cells throughout the range of frequencies studied (typical cell shortening records are shown in Figure 1, upper panel). The shapes of the shortening-frequency relationships from 2 to 10 Hz were similar in both experimental groups (Fig. 1, lower panel). However, after inhibition of NHE-1 with HOE 694, fractional shortening in the heart failure group was significantly depressed (by approx. 22%). Moreover, the shape of the shortening-frequency relationship was altered. Maximal shortening was observed at 5 Hz after NHE-1 inhibition, while normally peak shortening was observed at 7 Hz. HKA inhibition with SCH 28080 did not affect fractional shortening, indicating that this exchanger mechanism is not significantly activated under the present conditions (data not shown).

As shown in Figure 2, pH_i was chronically reduced in heart failure myocytes, by approx. 0.07 pH units. Moreover, pH_i progressively decreased with increased pacing frequency in both sham and heart failure groups, whereas NHE-1 inhibition decreased pH_i by approx. 0.03 pH-units in control and approx. 0.05 pH-units in heart failure, respectively. In controls, the difference between normal and NHE-1-inhibited cells reached statistical significance only at 2 Hz; P -values for 5–10 Hz ranged 0.073–0.11 (Mann–Whitney test). However, repeated-measures ANOVA analysis concluded difference between control cells with or without NHE-1 blockade, as well as between failing cells with or without NHE-1 blockade. Inhibiting the HKA did not affect pH_i , indicating no significant role for pH_i regulation under the present conditions (data not shown).

Table 2 Body mass, heart weights and cardiomyocyte size

	Control	Heart failure
Body mass (g)	260 \pm 22	280 \pm 25
Heart weight		
mg	1327 \pm 131	1734 \pm 208*
mg g ⁻¹	5.1 \pm 0.2	6.2 \pm 0.8*
LV weight		
mg	1019 \pm 80	1358 \pm 150*
mg g ⁻¹	3.9 \pm 0.2	4.9 \pm 0.7*
RV weight		
mg	308 \pm 35	376 \pm 59**
mg g ⁻¹	1.2 \pm 0.1	1.3 \pm 0.2
LV cardiomyocyte length (μm)	100.8 \pm 3.0	123.3 \pm 4.5*
LV cardiomyocyte width (μm)	16.3 \pm 1.0	21.5 \pm 1.9*
LV cardiomyocyte volume (pL)	12.5 \pm 1.0	20.1 \pm 2.1*

Data are mean \pm SD, $n = 11$ in each group; 100 cells from each rat were measured for cellular dimensions.

LV, left ventricle; RV, right ventricle.

Differences between control and heart failure: * $P < 0.01$;

** $P < 0.05$.

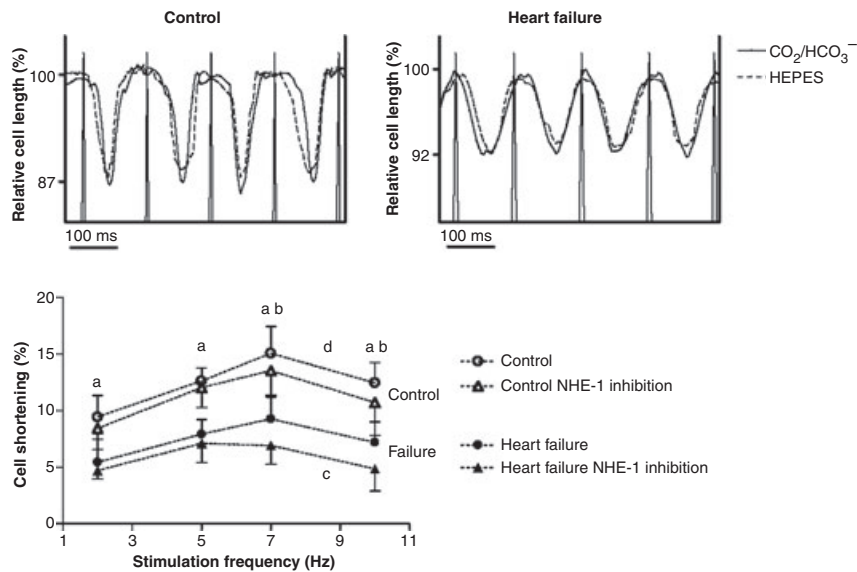


Figure 1 Cardiomyocyte fractional shortening. Upper panel shows typical cell shortening traces at 7 Hz stimulation with cells either in CO₂/HCO₃⁻ or HEPES-buffered Tyrode; no differences occurred between CO₂/HCO₃⁻ and HEPES solutions. Lower panel shows fractional shortening during increasing stimulation frequencies in control and heart failure, either in only CO₂/HCO₃⁻ Tyrode vehicle or also with the selective Na⁺/H⁺ exchanger-1 (NHE-1) inhibitor HOE 694. Inhibition with the selective H⁺/K⁺ ATPase (HKA) inhibitor SCH 28080 had no effect (data not shown). Data are mean ± SD, *n* = 7 in each group; four to six cells per animal in each condition. Differences between Control vs. Heart failure, and Control NHE-1 inhibition vs. Heart failure NHE-1 inhibition: a *P* < 0.01; differences between Heart failure vs. Heart failure NHE-1 inhibition: b *P* < 0.05 (Mann–Whitney test). Deviating curve-shape (staircase) between Heart failure vs. Heart failure NHE-1 inhibition: c *P* < 0.01; between Control vs. Control NHE-1 inhibition: d *P* < 0.05 (repeated-measures ANOVA).

Within each stimulation frequency, fractional shortening and pH_i correlated well with each other, most notably at physiological frequencies (7–10 Hz). Pearson's correlation coefficient was 0.444 (*P* < 0.01), 0.371 (*P* < 0.05), 0.604 (*P* < 0.01), and 0.647 (*P* < 0.01), for 2, 5, 7 and 10 Hz respectively (Fig. 3). Note the rightward shift with increasing pacing frequencies and the distinction between sham and heart failure.

Backward multiple regression suggested LVEDP as an important determinant for fractional shortening; unstandardized coefficient *b* −0.299 ± SE 0.069, *P* < 0.01, residual SD = 2.29, and adjusted *R*² = 0.58. However, the degree of heart failure (LVEDP) did not correlate with pH_i in this cohort. A detailed analysis of a potential relationship would require a larger variation in the severity of heart failure than in the present study.

Heart failure attenuated the rate of contraction and relaxation in cardiomyocytes (Table 3). Neither NHE-1 nor HKA inhibition affected contraction or relaxation rates.

To study whether or not HCO₃⁻ buffer systems may account for any of the observed changes in contractility or pH_i in the present study, experiments were repeated with the cells in HEPES-buffered Tyrode, i.e. in the absence of HCO₃⁻. No differences were found between experiments conducted in HCO₃⁻ or HEPES solutions (Figs 1 and 2).

Discussion

The novelty of the present study is the observation of lower pH_i in cardiomyocytes isolated from hearts with post-MI heart failure. The acidosis is closely correlated with reduced contractile function in the cell. Reduced contractility in response to reduced pH_i has consistently been shown in experiments acutely altering acid load (for review, see Orchard & Kentish 1990), and appears as a complex sum of several factors, including myofilament Ca²⁺ sensitivity, electrical activity and intracellular Ca²⁺ handling. Concordant depression of pH_i and contractility after blockade by HOE 694 indicates that NHE-1 may act as a significant mechanism to compensate for increased intracellular acid load. Similar results obtained in experiments exchanging HCO₃⁻-buffered Tyrode with HEPES-buffered Tyrode suggests that HCO₃⁻-buffer systems do not account for the reduced pH_i in heart failure. Chronically, reduced myocardial pH_i has previously been reported in pressure-overload hypertrophy (Wallis *et al.* 1997) but not in heart failure.

Reduced pH_i in heart failure

Currently, the cellular mechanism underlying the lower pH_i in HF is unknown. One possibility is that there is a

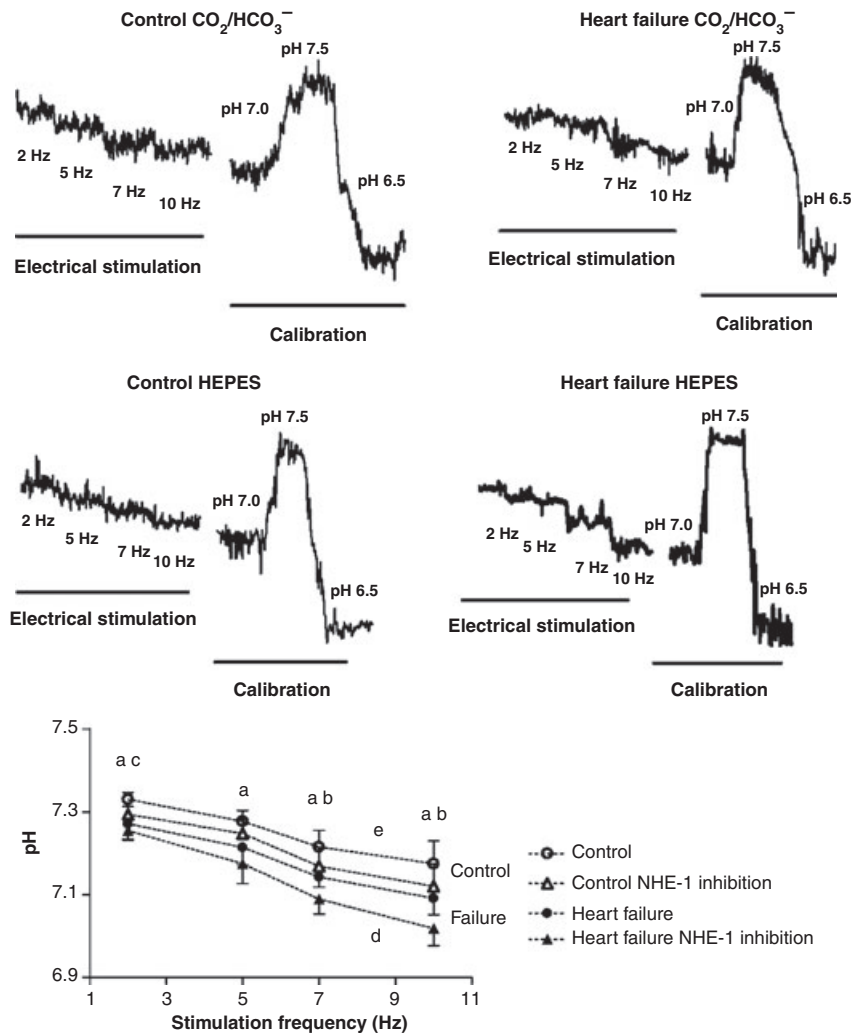


Figure 2 Cardiomyocyte intracellular pH. Upper four panels show typical pH traces during 2–10 Hz stimulation with cells either in CO₂/HCO₃⁻ or HEPES-buffered Tyrode, and nigericin calibration. No differences occurred between CO₂/HCO₃⁻ and HEPES solutions; to distinguish traces from the two Tyrode solutions, traces are displayed separately. Bottom panel shows pH during increasing stimulation frequencies in control and heart failure, either in Tyrode vehicle or with the selective Na⁺/H⁺ exchanger-1 (NHE-1) inhibitor HOE 694. Inhibition with the selective H⁺/K⁺ ATPase (HKA) inhibitor SCH 28080 had no effect and is thus not shown. Data are mean ± SD, *n* = 7 in each group; four to six cells per animal in each condition. Differences between Control vs. Heart failure, and Control NHE-1 inhibition vs. Heart failure NHE-1 inhibition: a *P* < 0.01; differences between Heart failure vs. Heart failure NHE-1 inhibition: b *P* < 0.01; differences between Control and Control NHE-1 inhibition: c *P* < 0.01 (Mann–Whitney test). Deviating curve-shape (staircase) between Heart failure vs. Heart failure NHE-1 inhibition: d *P* < 0.01; between Control vs. Control NHE-1 inhibition: e *P* < 0.05 (repeated-measures ANOVA).

chronic increase in acid load. In heart failure, there is thought to be a shift towards more anaerobic metabolism and increased cytoplasmic acid load. This may act to reduce pHi (Ventura-Clapier *et al.* 2004). However, earlier work indicates that increased lactic acid production by itself would cause a transient, not a sustained change of pHi (Eisner *et al.* 1993). The presence of a sarcolemmal lactic acid transporter and intracellular pH regulation ensures that the steady state pHi is regulated back to control values. A second possibility is that intracellular pH set-point has been altered by changes in

the relative status of the pH regulatory mechanisms. The most likely candidate for this mechanism is altered NHE activity since the pH differential was also present in HEPES buffered solutions. Raised intracellular Na⁺ levels have been reported for several animal models of hypertrophy and heart failure (Gray *et al.* 2001, Despa *et al.* 2002). This change alone would reduce the effectiveness of the NHE and result in an acid shift in intracellular pH. Further work is required to test this hypothesis and further establish the cellular mechanism underlying the altered intracellular pH in heart failure.

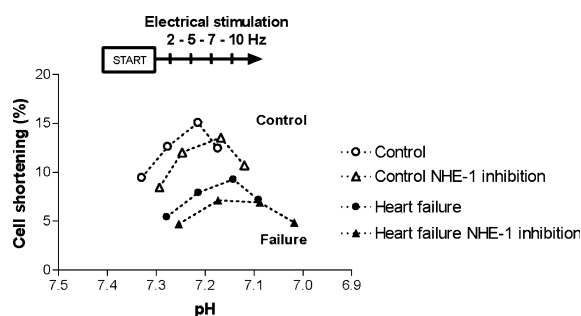


Figure 3 Relationship between fractional shortening and intracellular pH. Control and Heart failure groups are plotted, including those that received selective Na^+/H^+ exchanger-1 (NHE-1) inhibitor with HOE 694. Inhibition with the selective H^+/K^+ ATPase (HKA) inhibitor SCH 28080 had no effect (data not shown). SD was removed as they are presented in Figures 2 and 3, from which data are integrated and re-plotted (2–10 Hz).

Table 3 Cardiomyocyte contraction and relaxation times at 7 Hz

	Control	Heart failure
Relative time to peak contraction (ms FS^{-1})		
Vehicle	3.9 ± 0.6	$7.0 \pm 1.8^*$
NHE-1 inhibition	4.6 ± 1.3	$9.2 \pm 1.8^*$
HKA inhibition	3.8 ± 0.4	$6.8 \pm 1.2^*$
Time to peak contraction (ms)		
Vehicle	58 ± 4	$62 \pm 4^{**}$
NHE-1 inhibition	59 ± 4	61 ± 7
HKA inhibition	56 ± 5	62 ± 6
Time to 50% contraction (ms)		
Vehicle	38 ± 3	$44 \pm 2^*$
NHE-1 inhibition	41 ± 5	45 ± 3
HKA inhibition	38 ± 3	$44 \pm 4^*$
Time to 50% relaxation (ms)		
Vehicle	48 ± 4	$57 \pm 2^*$
NHE-1 inhibition	51 ± 7	$58 \pm 3^{**}$
HKA inhibition	49 ± 3	$58 \pm 4^*$

Data are mean \pm SD, $n = 11$ in each group, four to six cells per animal in each condition.

FS, fractional shortening; Vehicle, physiological $\text{CO}_2/\text{HCO}_3^-$ -buffered Tyrode solution; NHE-1 inhibition, selective Na^+/H^+ exchanger 1 inhibition with HOE 694; HKA inhibition, selective H^+/K^+ ATPase inhibition with SCH 28080. Note the trend to prolonged relative contraction time after NHE-1 inhibition in both control and heart failure cardiomyocytes. Experiments were also repeated in HEPES-buffered Tyrode for all conditions; no differences were revealed between $\text{CO}_2/\text{HCO}_3^-$ - and HEPES-buffered Tyrode solutions.

Differences between control and heart failure: $*P < 0.01$;

$**P < 0.05$.

The increased intracellular proton concentration in HF will interfere with Ca^{2+} binding to the troponin complex and thus shift the dependence of actomyosin

ATPase and tension generation to higher Ca^{2+} concentrations (Blanchard & Solaro 1984, Orchard & Kentish 1990, Hulme & Orchard 1998). Therefore, the lower pH_i in heart failure would be expected to reduce Ca -activated contractility. In line with this, it was recently reported that the failing heart becomes more acidic than normal hearts when challenged by ischaemia. The greater drop in pH_i was caused by a compromised ability to take up and utilize glucose and free fatty acids. Thus, substrate starvation is compensated by ATP hydrolysis from break-down of glycogen, but this also increases proton production (Murray *et al.* 2006).

pH_i , Ca^{2+} and contractility

Despite maintained or increased cardiomyocyte Ca^{2+} transients in heart failure (Loennechen *et al.* 2002, Wisløff *et al.* 2002); a common feature is depressed contractile function (Perez *et al.* 1999, Zhang *et al.* 1999). Reduced myofilament Ca^{2+} sensitivity may reduce cell function in heart failure, as reported in some experimental models (Perez *et al.* 1999, Loennechen *et al.* 2002, Wisløff *et al.* 2002), although it is not a uniform observation (Gwathmey & Hajjar 1990, Hajjar *et al.* 2000). Accumulated evidence suggests that myocardial pH_i regulation, Ca^{2+} sensitivity and contractility are linked entities in both normal and failing hearts (Wisløff *et al.* 2001, 2002), whereas a drop in pH_i results in a rightward shift in the Ca^{2+} -force curve of both skinned and intact cardiomyocytes; thus, a lower Ca^{2+} sensitivity (Fabiato & Fabiato 1978, Orchard & Kentish 1990). Taken together, the present study and previous observations indicate that the positive staircase from 2 to 7 Hz may be due to increased Ca^{2+} transients, whereas above 7 Hz, the staircase turns negative due to decreased pH_i in failing cells that negatively affects Ca^{2+} sensitivity. However, acidosis may also affect cell membrane currents, action potential duration and intracellular Ca^{2+} handling (Orchard & Kentish 1990).

NHE-1, pH_i , Ca^{2+} and contractility

Several lines of evidence indicate that NHE-1 contributes to the maintenance of pH_i and cardiomyocyte contractility. In heart failure, NHE-1 expression is markedly increased (Karmazyn *et al.* 1999, Loennechen *et al.* 2002). Reduced myocyte pH_i and contractility occur after blockade by HOE 694, indicating that compensatory potential depends critically on its transport capacity. As described above, the contractile response at increasing contraction rates is influenced by H^+ extrusion as well as accompanying changes in intracellular Na^+ and Ca^{2+} concentrations. In heart failure, increased tendency towards anaerobic

metabolism and H⁺ production (Ventura-Clapier *et al.* 2004) may stimulate NHE-1 transport capacity and lead to a negative staircase at lower contraction rates. A transition from positive to negative staircase may have important negative clinical consequences, since it translates into a mismatch between cardiac pump capacity and peripheral demand. In this study, acute inhibition of NHE-1 depressed contractile function, in contrast to chronic inhibition of NHE-1 that is cardio-protective in heart failure and cardiac hypertrophy, as pathologic remodelling is attenuated. This may not be related to pH_i, but to reduced Na⁺ entry and altered ion balance, which would affect various cell signalling mechanisms such as protein kinase C and mitogen-activated protein kinases (Karmazyn *et al.* 1999). Besides NHE-1, MCT-1 (Johannsson *et al.* 2001) and HKA (Beisvag *et al.* 2003) may also act to maintain optimal pH_i in heart failure. However, our data do not support any role of HKA, which requires a markedly lower pH_i for activation (Beisvag *et al.* 2003). We could also not detect any role of HCO₃⁻-buffer systems for chronically changed pH_i, in contrast to the finding that electrogenic Na⁺-HCO₃⁻ cotransport increases as the rate of stimulation, and hence depolarization, increases, which results in elevated HCO₃⁻ influx, and thus an improved ability to buffer H⁺ in the HCO₃⁻-perfused heart (Camilion de Hurtado *et al.* 1996). Methodological differences may explain this discrepancy.

Conclusion

Reduced cardiomyocyte pH_i and insufficient proton extrusion by NHE-1 was observed in myocytes from failing rat hearts. The acidic intracellular pH will contribute to the reduced contractility observed in this HF model.

Conflicts of interest

No conflicts of interest exist.

This study was supported by research grants from the SINTEF Unimed, the National Council on Cardiovascular Diseases, the St Olavs Hospital, and the Torstein Erbo, Arild and Emilie Bachke, EWS, and Agnes Sars Foundations. Ole Johan Kemi was the recipient of a research fellowship from the Norwegian University of Science and Technology.

References

Beisvag, V., Falck, G., Loennechen, J.P. *et al.* 2003. Identification and regulation of the gastric H⁺/K⁺-ATPase in the rat heart. *Acta Physiol Scand* **179**, 251–262.

Blanchard, E.M. & Solaro, R.J. 1984. Inhibition of the activation and troponin calcium binding of dog cardiac myofibrils by acidic pH. *Circ Res* **55**, 382–391.

Brixius, K., Reicke, S. & Schwinger, R.H.G. 2002. Beneficial effects of the Ca²⁺ sensitizer levosimendan in human myocardium. *Am J Physiol Heart Circ Physiol* **282**, H131–H137.

Camilion de Hurtado, M.C., Alvarez, B.V., Perez, N.G. & Cingolani, H.E. 1996. Role of an electrogenic Na⁺-HCO₃⁻ cotransport in determining myocardial pH_i after an increase in heart rate. *Circ Res* **79**, 698–704.

Chen, L., Chen, C.X., Gan, X.T., Beier, N., Scholz, W. & Karmazyn, M. 2004. Inhibition and reversal of myocardial infarction-induced hypertrophy and heart failure by NHE-1 inhibition. *Am J Physiol Heart Circ Physiol* **286**, H381–H387.

Despa, S., Islam, M.A., Weber, C.R., Pogwizd, S.M. & Bers, D.M. 2002. Intracellular Na⁺ concentration is elevated in heart failure but Na/K pump function is unchanged. *Circulation* **105**, 2543–2548.

Eisner, D.A., Smith, G.L. & O'Neill, S.C. 1993. The effects of lactic acid production on contraction and intracellular pH during hypoxia in cardiac muscle. *Basic Res Cardiol* **88**, 421–429.

Fabiato, A. & Fabiato, F. 1978. Effects of pH on the myofilaments and the sarcoplasmic reticulum of skinned cells from cardiac and skeletal muscles. *J Physiol* **276**, 233–255.

Gray, R.P., McIntyre, H., Sheridan, D.S & Fry, C.H. 2001. Intracellular sodium and contractile function in hypertrophied human and guinea-pig myocardium. *Pflugers Arch Eur J Physiol* **442**, 117–123.

Gwathmey, J.K. & Hajjar, R.J. 1990. Relation between steady-state force and intracellular [Ca²⁺] in intact human myocardium. Index of myofibrillar responsiveness to Ca²⁺. *Circulation* **82**, 1266–1278.

Gwathmey, J.K., Slawsky, M.T., Hajjar, R.J., Briggs, G.M. & Morgan, J.P. 1990. Role of intracellular calcium handling in force-interval relationships of human ventricular myocardium. *J Clin Invest* **85**, 1599–1613.

Hajjar, R.J., Schwinger, R.H., Schmidt, U. *et al.* 2000. Myofilament calcium regulation in human myocardium. *Circulation* **101**, 1679–1685.

Hasenfuss, G., Pieske, B., Castell, M., Kretschmann, B., Maier, L.S. & Just, H. 1998. Influence of the novel inotropic agent levosimendan on isometric tension and calcium cycling in failing human myocardium. *Circulation* **98**, 2141–2147.

Hulme, J.T. & Orchard, C.H. 1998. Effect of acidosis on Ca²⁺ uptake and release by sarcoplasmic reticulum of intact rat ventricular myocytes. *Am J Physiol* **275**, H977–H987.

Johannsson, E., Lunde, P.K., Hedde, C. *et al.* 2001. Upregulation of the cardiac monocarboxylate transporter MCT1 in a rat model of congestive heart failure. *Circulation* **104**, 729–734.

Karmazyn, M., Gan, X.T., Humphreys, R.A., Yoshida, H. & Kusumoto, K. 1999. The myocardial Na⁺-H⁺ exchange: structure, regulation, and its role in heart disease. *Circ Res* **85**, 777–786.

Leem, C.H., Lagadic-Gossman, D. & Vaughan-Jones, R.D. 1999. Characterization of intracellular pH_i regulation in the guinea-pig ventricular myocyte. *J Physiol* **517**, 159–180.

Lehmann, A., Boldt, J. & Kirchner, J. 2003. The role of Ca²⁺ sensitizers for the treatment of heart failure. *Curr Opin Crit Care* **9**, 337–344.

- Litwin, S.E., Katz, S.E., Morgan, J.P. & Douglas, P.S. 1994. Serial echocardiographic assessment of left ventricular geometry and function after large myocardial infarction in the rat. *Circulation* **89**, 345–354.
- Loennechen, J.P., Støylen, A., Beisvag, V., Wisløff, U. & Ellingsen, Ø. 2001. Regional expression of endothelin-1, ANP, IGF-1, and LV wall stress in the infarcted rat heart. *Am J Physiol Heart Circ Physiol* **280**, H2902–H2910.
- Loennechen, J.P., Wisløff, U., Falck, G. & Ellingsen, Ø. 2002. Effects of cariporide and losartan on hypertrophy, calcium transients, contractility, and gene expression in congestive heart failure. *Circulation* **105**, 1380–1386.
- Murray, A.J., Lygate, C.A., Cole, M.A. et al. 2006. Insulin resistance, abnormal energy metabolism and increased ischemic damage in the chronically infarcted rat heart. *Cardiovasc Res* **71**, 149–157.
- Nagashima, R., Tsuda, Y., Maruyama, T., Kanaya, S., Fujino, T. & Niho, Y. 1999. Possible evidence for transmembrane K⁺–H⁺ exchange system in guinea pig myocardium. *Jpn Heart J* **40**, 351–364.
- Orchard, C.H. & Kentish, J.C. 1990. Effects of changes of pH on the contractile function of cardiac muscle. *Am J Physiol* **258**, C967–C981.
- Perez, N.G., Hashimoto, K., McCune, S., Altschuld, R.A. & Marban, E. 1999. Origin of contractile dysfunction in heart failure; calcium cycling vs. myofilaments. *Circulation* **99**, 1077–1083.
- Satoh, H., Delbridge, L.M., Blatter, L.A. & Bers, D.M. 1996. Surface:volume relationship in cardiac myocytes studied with confocal microscopy and membrane capacitance measurements: species-dependence and developmental effects. *Biophys J* **70**, 1494–1504.
- Teshima, Y., Akao, M., Jones, S.P. & Marban, E. 2003. Cariporide (HOE 642), a selective Na⁺–H⁺ exchange inhibitor, inhibits the mitochondrial death pathway. *Circulation* **108**, 2275–2281.
- Ventura-Clapier, R., Garnier, A. & Veksler, V. 2004. *Energy metabolism in heart failure*. *J Physiol* **555**, 1–13.
- Wallis, W.R., Wu, C., Sheridan, D.J. & Fry, C.H. 1997. Intracellular pH and H⁺ buffering capacity in guinea-pigs with left ventricular hypertrophy induced by constriction of the thoracic aorta. *Exp Physiol* **82**, 227–230.
- Wisløff, U., Loennechen, J.P., Falck, G. et al. 2001. Increased contractility and calcium sensitivity in cardiac myocytes isolated from endurance trained rats. *Cardiovasc Res* **50**, 495–508.
- Wisløff, U., Loennechen, J.P., Currie, S., Smith, G.L. & Ellingsen, Ø. 2002. Aerobic exercise reduces cardiomyocyte hypertrophy and increases contractility, Ca²⁺ sensitivity and SERCA-2 in rat after myocardial infarction. *Cardiovasc Res* **54**, 162–174.
- Yenisehirli, A. & Onur, R. 2005. Positive inotropic and negative chronotropic effects of proton pump inhibitors in isolated rat atrium. *Eur J Pharmacol* **519**, 259–266.
- Zaniboni, M., Swietach, P., Rossini, A., Yamamoto, T., Spitzer, K.W. & Vaughan-Jones, R.D. 2003. Intracellular proton mobility and buffering power in cardiac ventricular myocytes from rat, rabbit, and guinea pig. *Am J Physiol Heart Circ Physiol* **285**, H1236–H1246.
- Zhang, X.Q., Musch, T.I., Zelis, R. & Cheung, J.Y. 1999. Effects of impaired Ca²⁺ homeostasis on contraction in postinfarction myocytes. *J Appl Physiol* **86**, 943–950.